

# Air4EU

**Air Quality Assessment for Europe: from local to continental scale**



6th Framework Programme- Policy oriented Research  
Priority 8.1 Topic 1.5 Task 2

## **Individual case study report 6: Basic data assimilation: application to the urban scale**

Deliverable:	D7.1 Part 6
Dissemination level:	PU
Editor:	Bruce Denby
Version:	Final
Date:	March 2007
Contract:	503596

## LIST OF AIR4EU PARTNERS

<b>Partic. no.</b>	<b>Participant name</b>	<b>Participant short name</b>	<b>Country</b>
1	Netherlands Research Organisation	TNO	NL
2	Norsk Institut for Luftforskning	NILU	NO
3	Aristotle University Thessaloniki	AUT	GR
4	University of Stuttgart	IER	DE
5	University of Hertfordshire	UH	UK
6	Universidade de Aveiro	UAVR	PT
7	AIRPARIF	AIRPARIF	FR
8	Agenzia per i Trasporti Autoferrotramviari e la Mobilità del Comune di Roma S.p.A.	ATAC	IT
9	Environment Agency	EA	UK
10	City Development Authority of Prague	URM	CZ
11	Enveco	ENVECO	GR
12	Gemeentewerken Rotterdam	GW	NL
13	Milieudienst Rijnmond	DCMR	NL
14	City of Oslo, Public Health Authority	OPHA	NO



## Table of Content

<b>1. Executive Summary</b> .....	<b>2</b>
<b>2. Case study description</b> .....	<b>2</b>
2.1 Background.....	2
2.2 Aim and description .....	2
2.3 Relevance to recommendations in Air4EU .....	3
<b>3. Methodology</b> .....	<b>3</b>
3.1 The ATEM model.....	4
3.2 The observations .....	5
3.3 Assessment of the results.....	7
3.4 Assimilation methods .....	7
3.4.1 Linear regression.....	7
3.4.2 Ordinary kriging .....	8
3.4.3 Ordinary kriging of the residual .....	9
3.4.4 Bayesian assimilation of kriged and model fields.....	9
3.5 Uncertainty mapping .....	10
3.5.1 RME as an uncertainty parameter.....	10
3.5.2 Spatial interpolation of RME .....	11
3.5.3 Indicative RMSE .....	11
3.5.4 Kriging and assimilation uncertainty fields .....	12
3.5.5 Cross validation of the observational mean and the RMSE.....	12
3.6 Probability of exceedance maps.....	12
<b>4. Results</b> .....	<b>13</b>
4.1 Statistical analysis of model and observations .....	13
4.2 Linear regression.....	14
4.3 Kriging of observations .....	16
4.4 Kriging of the observed – modelled residual .....	18
4.5 Bayesian combination of the observed and modelled fields.....	19
4.6 Summary of the assimilation methods.....	20
4.7 Final set of concentration and uncertainty maps .....	21
4.8 Mapping of RME as an uncertainty indicator .....	25
4.9 Probability of exceedance maps.....	27
<b>5. Conclusion and discussion</b> .....	<b>28</b>
5.1 Assessment of the case study .....	28
5.2 Improvements in assessment derived from case study.....	28
5.3 Recommendations resulting from the case study .....	29
5.4 Suitability for implementation in other cities .....	29
<b>References</b> .....	<b>29</b>

## **1. Executive Summary**

There are a number of methodologies available for combining monitoring and modelling data that will lead to the production of maps showing air quality. Many of these are complex applications involving data assimilation techniques that will require direct interaction between model calculations and observational data. The complexity of such methods limits their application to research institutes, making them inaccessible to city authorities that require such maps. This case study looks at a number of 'off line' methods for combining maps of annual means, calculated using a Gaussian statistical model, with monitoring data. The application area is the city of Prague where data from 12 monitoring stations measuring the pollutants PM<sub>10</sub>, SO<sub>2</sub> and NO<sub>2</sub> are available. The assimilation methods investigated include regression analysis, kriging, kriging of the observed-modelled residual and Bayesian assimilation. The quality of the assimilation method is assessed using the cross validation RMSE. The results of the study show that all of the assimilation methods for this application can provide improved maps of air quality with the general conclusion that regression analysis is the simplest and most effective method for improving the maps and their associated uncertainty. Small improvements can be achieved through residual kriging and through Bayesian assimilation of kriged observational fields. The major improvement obtained with all the methods is through the removal of model bias. To demonstrate the improvements in the air quality maps, corresponding uncertainty maps are also produced along with maps indicating the probability of exceedance. The case study supports a number of recommendations concerning combining monitoring and modelling on the urban scale.

## **2. Case study description**

### **2.1 Background**

There are a number of methodologies available for combining monitoring and modelling data. Many of these are complex applications involving data assimilation techniques that require direct interaction between model calculations and observed data. Examples of these are variational methods, e.g. 4D var, Kalman filters and other particle filter methods, see the cross cutting issue report on data assimilation (Air4EU – M5) for references to current applications and references. There are also other methods that can be applied 'offline' where precalculated model fields can be adjusted using monitoring data. These methods do not require interaction with the model and make use solely of the resulting fields. Examples of such methods are 3D var, optimal interpolation, regression modelling and various kriging methods. Such methods are easier to implement without having to interact with complex models and some of these can be implemented using standard software. Such methods can be applied to any field with no temporal dimension. Examples of these are model calculations of annual means and other air quality indicators that can be both modelled and monitored.

As part of Air4EU these simpler methods are also explored in two case studies; this case study, which looks at their application on the urban scale, and the Europe II case study (Air4EU – CS D7.1.13) that looks at their application on the regional scale. In addition the Paris case study (Air4EU – CS D7.1.7) also applies one of these types of methods. Other applications using similar statistical methods, such as kriging and regression, include Kassteele et al. (2006), Horálek et al. (2005), Denby and Flicstein (2005), Yuval and Broday (2006) and Blond et al. (2003).

### **2.2 Aim and description**

The aim of this case study is to apply and test basic data assimilation methodologies that can be used to combine monitoring and models to improve precalculated model fields and produce more reliable

maps of concentrations for urban regions. Preexisting maps of annual mean concentrations produced for the city of Prague using the ATEM model (Brechler, 2000) for PM<sub>10</sub>, SO<sub>2</sub> and NO<sub>2</sub> will be used in combination with 12 monitoring sites located within the city of Prague.

A number of methods will be tested and the results will be objectively assessed using the cross-validation root mean square error (RMSE). The methods tested include

- Linear regression of the model fields
- Ordinary kriging of the observed fields
- Kriging of the residual fields (observed – model)
- Bayesian combination of kriged observations and model fields

In addition to the maps of concentrations fields the uncertainty of the maps will be discussed and maps showing uncertainty will be displayed. These will be based on a number of different parameters and methods including

- Spatial maps of the RME (Relative maximum error)
- Spatial maps of the RMSE based on estimated model uncertainty
- Spatial maps based on uncertainty in the kriging interpolation
- Spatial maps based on the combined uncertainty of model and observed fields
- Spatial maps showing the probability of exceedance

The aim is to assess the usefulness of the assimilation methods and uncertainty mapping when applied to urban areas.

## **2.3 Relevance to recommendations in Air4EU**

Air4EU intends to provide recommendations on spatial assessment for a range of users including city authorities. If data assimilation techniques are to be implemented by these authorities then they must be operationally applicable and, unless research institutes active in data assimilation are engaged in the assessment, they must also be based on accessible technologies. For this reason it is important to explore and recommend methodologies for data assimilation that can lead to improved spatial assessment using basic and available methods.

This case study tests a number of such methodologies that can be applied to urban scales. It will lead to recommendations concerning the use of such methods for air quality assessment as well as exploring methodologies for displaying the uncertainty in these fields.

## **3. Methodology**

As previously mentioned a number of methodologies will be applied to available maps from the ATEM model, a statistical Gaussian model applied in Prague. The pollutants and indicators investigated will be:

- PM<sub>10</sub> annual mean
- SO<sub>2</sub> annual mean
- NO<sub>2</sub> annual mean

### 3.1 The ATEM model

The ATEM model is a statistical Gaussian model that produces annual mean pollutant fields at a resolution of 250 m for the city of Prague. The model is originally based on the US EPA model IST2. Emissions for the model include point, line and area sources within the model regions as well as a number of point sources external to that region. A set of statistical wind roses and stability classes are used for the calculation based upon results from a local mesoscale model. More information concerning the model can be found in Brechler (2000).

In the figures below the calculated model fields for the year 2003 are presented along with the observations, shown as circles, with their value given in text ( $\mu\text{g}/\text{m}^3$ ). The colour scales vary from compound to compound but the same scale will be used throughout the rest of the paper in regard to the assimilated fields for each compound.

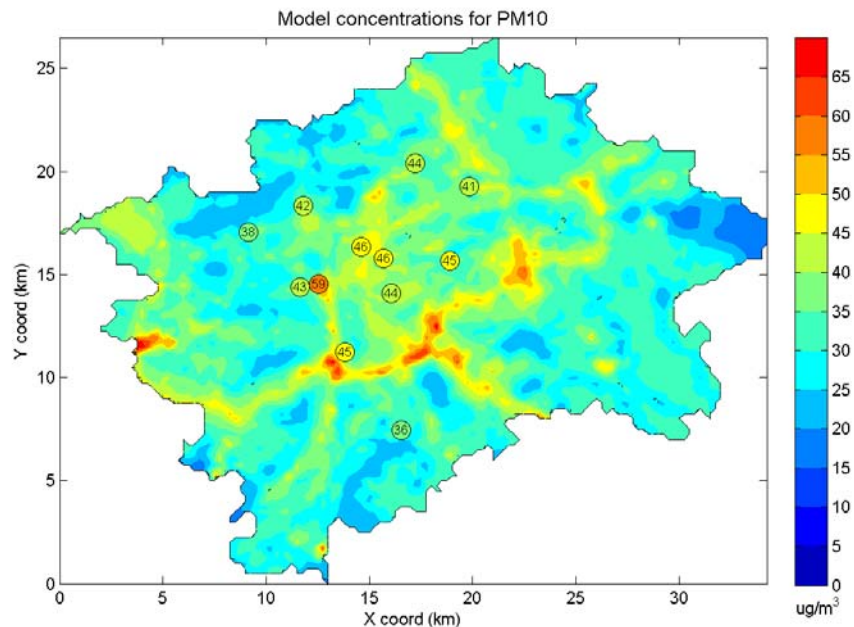


Figure 3.1: Modelled, filled contours, and observed, circles with values, annual mean concentrations ( $\mu\text{g}/\text{m}^3$ ) for  $\text{PM}_{10}$  in Prague 2003. Model field as calculated by the ATEM model.

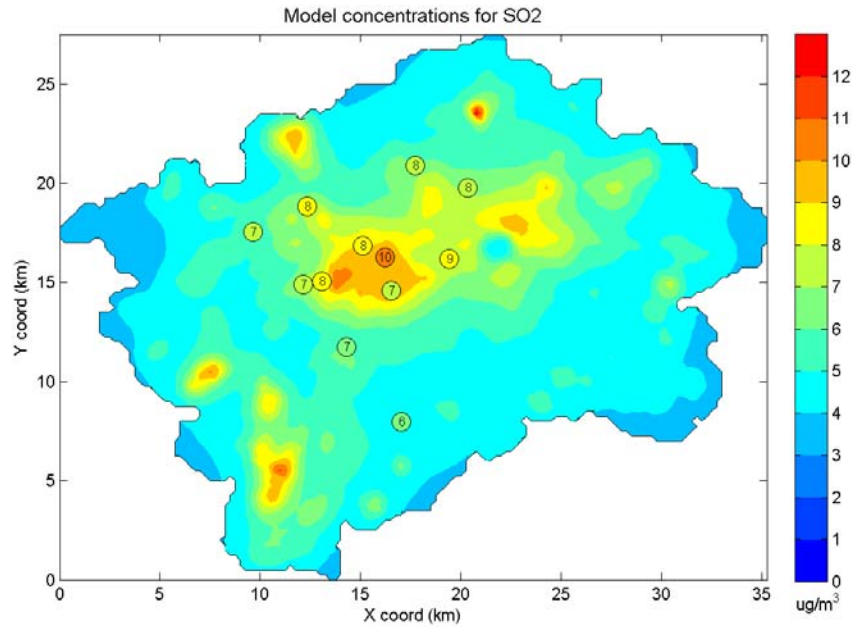


Figure 3.2: Modelled, filled contours, and observed, circles with values, annual mean concentrations ( $\mu\text{g}/\text{m}^3$ ) for  $\text{SO}_2$  in Prague 2003. Model field as calculated by the ATEM model.

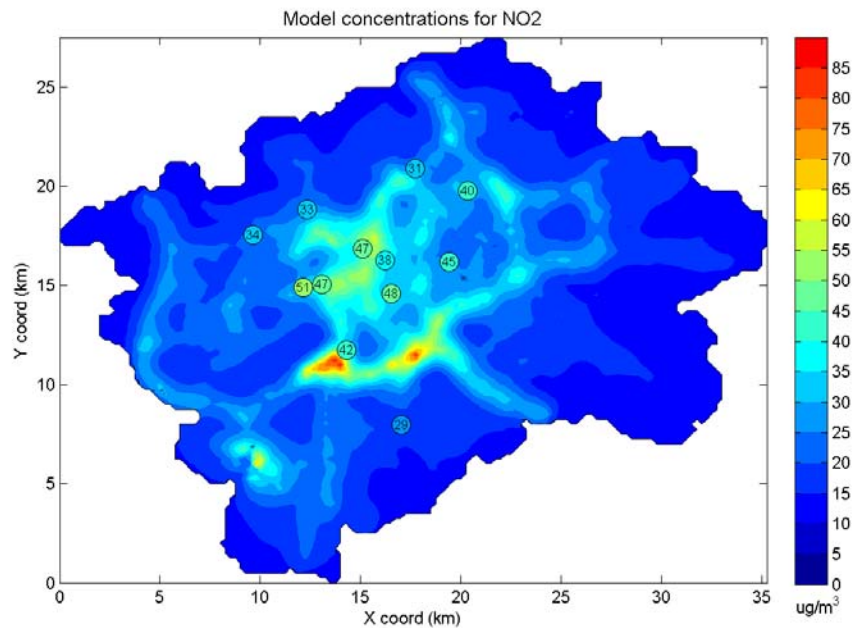


Figure 3.3: Modelled, filled contours, and observed, circles with values, annual mean concentrations ( $\mu\text{g}/\text{m}^3$ ) for  $\text{NO}_2$  in Prague 2003. Model field as calculated by the ATEM model

### 3.2 The observations

12 monitoring stations are available for the calculations. Their positions are shown in the map below.

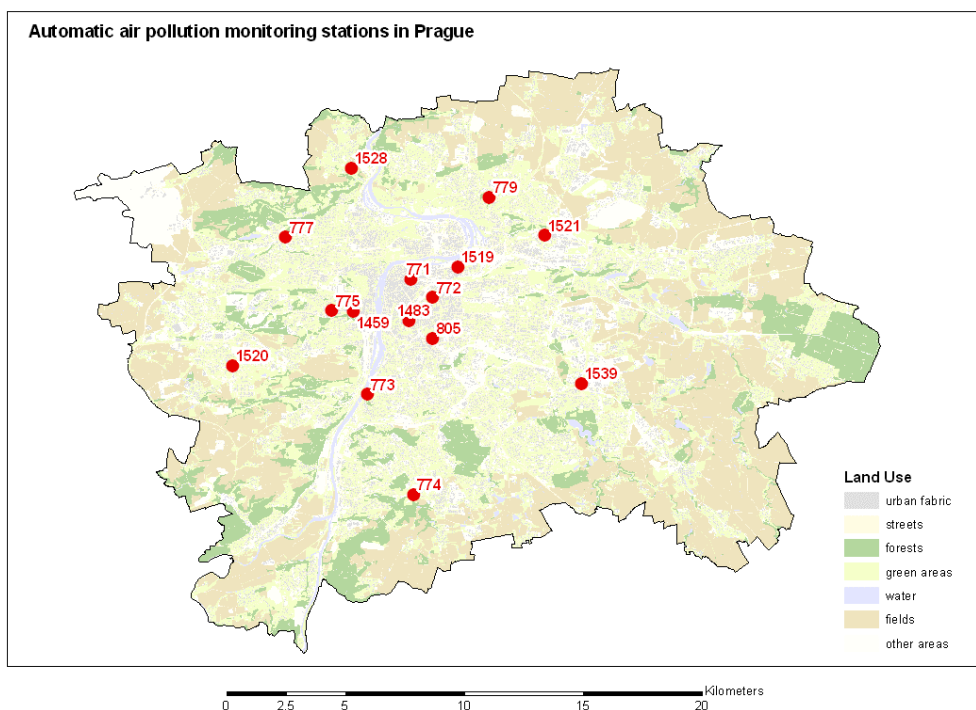


Figure 3.1: Position of monitoring stations in Prague. Not all stations shown in the figure have been used, see table 3.1 for details.

The stations used are assumed to be representative of the modelling scale, that being of a 250 x 250 m region surrounding the monitoring station. Unknown representativeness errors will occur as a result of this assumption.

Table 3.1: Annual mean values for  $PM_{10}$ ,  $SO_2$  and  $NO_2$  for the stations used in the study.

STATION CODE	STATION NUMBER	Annual mean $NO_2$ ( $\mu\text{g}/\text{m}^3$ )	Annual mean $PM_{10}$ ( $\mu\text{g}/\text{m}^3$ )	Annual mean $SO_2$ ( $\mu\text{g}/\text{m}^3$ )
AREPA	771	47.24	46.41	8.42
ARIEA	772	37.698	45.61	10.45
ABRAA	773	41.6	45.18	6.68
ALIBA	774	28.66	35.7	6.42
AMLYA	775	50.97	42.68	7.27
ASMIA	1459	47.38	58.58	8.37
ASANA	776	32.92	41.72	8.11
AVELA	777	33.85	37.77	7.27
AKOBA	779	31.46	44.25	7.74
AVYCA	780	40.25	40.6	7.64
APOCA	804	44.85	45.32	8.91
AVRSA	805	47.8	43.58	7.38

### 3.3 Assessment of the results

In order to assess the results a number statistical parameters are used. Central to the assessment, as well as the determination of uncertainty, is the use of cross validation as a comparative test. Cross validation involves carrying out the assimilation using all the observations except one. The excluded observation is compared to the calculated one and this process is rotated around all the observations. To give a single value assessment of the quality of the assimilation method the RMSE of the cross-validated errors is used.

To be consistent cross validation (CV) is used in all RMSE estimates. This includes the regression analysis as well as the kriging and kriging of residuals. In the case of regression it is expected, given a large enough observational dataset, that the CV RMSE and the total RMSE will be virtually equivalent. However in this case, with only 12 stations available, individual stations can have a significant effect on the CV RMSE and so this parameter is used.

### 3.4 Assimilation methods

The methodologies applied in the study are described in the following sections

#### 3.4.1 Linear regression

Linear regression can be used to produce regression models that relate model calculated concentrations to observed quantities. It is also possible to include other relevant fields, such as altitude, emissions, etc. in multiple regressions but in this study we will apply the regression model solely to the model calculated fields. Linear regression produces a result that minimises the RMSE between the regression model and the observations based on just 2 global parameters. This is written as

$$M_{LR} = a + bM$$

where  $M$  is the model field  $M_{LR}$  is the resulting linear regression field and  $a$  and  $b$  are the regression coefficients. In effect the entire model field is rescaled by the factor  $b$  (slope) and adjusted absolutely by the factor  $a$  (intercept). The intercept parameter  $a$  tells us something about the background concentrations but this will only be reliable when there is a high correlation in the regression. It is also useful in this regard to include stations that represent the regional background in the regression. Ideally, when applying such a regression, then a large number of observations should be used, covering a large range of concentrations and providing good correlation. However, most cities do not have a large number of monitoring stations with suitable spatial representativeness which can limit the applicability of the linear regression.

It is also possible to apply linear regression in a limited fashion. e.g. when there is high confidence in the regional background level the factor  $a$  can be specified and the regression only allowed to vary the slope  $b$ . In contrast, when the regional background value is poorly known and there is confidence in the model results then the slope can be held fixed at  $b = 1$  and the background value allowed to vary. This may often be the case for urban regions where regional background values are poorly defined and the number of measurement stations is limited.

Linear regression can be appropriate for models that have intrinsic bias in

- Total emissions
- Dispersion model formulations
- General estimates of wind speeds
- Background levels

However, linear regression is global in nature and will not help improve results when the variations are the result of:

- Local errors in emission factors
- Spatial variation in meteorological fields
- Local effects in wind, dispersion or emissions near monitoring sites

Because linear regression minimises the RMSE between model and observations it can easily be considered to always improve the model results. Of course this is not necessarily true, it's just that we do not know of any other results. For this reason cross-validation is also used on the linear regression to assess the usefulness of the method and to indicate its sensitivity to observations when these are limited in number.

### 3.4.2 Ordinary kriging

Kriging, in all its forms, is an often used interpolation method in the geosciences. It revolves around the assumption that there is spatial correlation between points in space that is related to the distance between the points, i.e. the closer the points are then the more correlated, the further away the less correlated. This spatial correlation is described by a spatial variance function, called the semi-variogram, that describes spatial variance as a function of distance, figure 3.2. This function can be used to interpolate to any point in space when other observations are available. The interpolation is carried out by weighting the nearby measurement points so that the variance at the interpolation point is minimised. In other words, given the assumed nature of the spatial variance function the value given to the interpolated point is statistically the most likely one. Defining the semi-variogram is thus critical to the method and should in principle be based on fits to the measured spatial variance, when sufficient observations are available. The weighting method is defined below where  $M_{OK}$  is the result of the ordinary kriging,  $\lambda_i$  is the weighting parameter and  $O(x_i, y_i)$  is the observation  $i$  at position  $x$  and  $y$ .

$$M_{OK}(x, y) = \sum_{i=1}^n \lambda_i O(x_i, y_i)$$

Kriging works best when the spatial variability is much larger than the distance between measurement points. As such it has been applied, in air quality applications, to a large number of ozone interpolation applications where the density of measurement stations is high in comparison to the spatial variability. In an urban setting where spatial variation is much finer in detail, kriging by itself is less likely to give useful results.

In this study only ordinary kriging is applied. This type of kriging is most often used. It separates itself from other kriging methods in that it requires the sum of the weights to be equal to 1. This leads to particular properties including that the interpolated field, far from the observations, approaches the mean of these observations. For a description of kriging methods one is referred to various books on the subject such as Webster and Oliver (2001) and Cressie (1993).

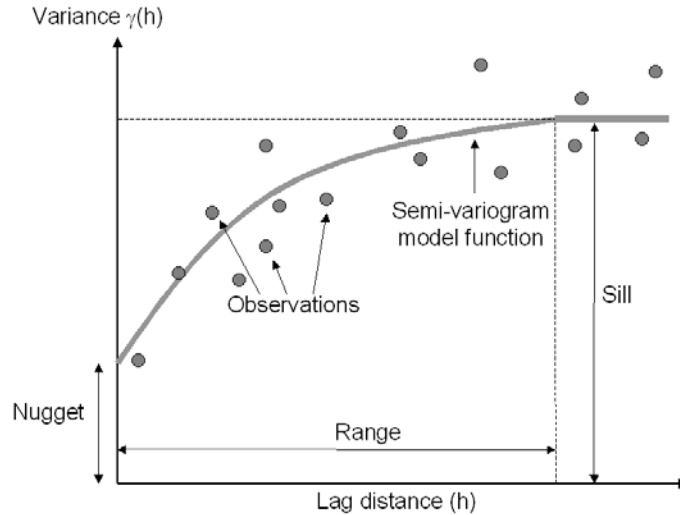


Figure 3.2: Showing the various parameters and terms used to describe the kriging semi-variogram function and how such a function can be fitted to the observed variance.

### 3.4.3 Ordinary kriging of the residual

Ordinary kriging assumes some form of stationarity to the field in as much that there are no spatial trends present. This is often not the case and so a number of methods for accounting for spatial trends, or 'external drift', can be applied. The method used here is to assume the model field represents the general character of the field, i.e. the drift, and to apply kriging to the residuals (also termed innovation), i.e. observations – model concentrations. This has been shown in other studies (Horelek, 2005; Blond et al., 2003) to be an effective method for improving mapped concentration fields on regional scales. The kriged field then becomes:

$$M_{OK\_RES}(x, y) = \left[ \sum_{i=1}^n \lambda_i (O(x_i, y_i) - M(x_i, y_i)) \right] + M(x, y)$$

In addition to kriging the residual it is also possible to apply kriging to the normalised residual and then multiply this with the model field. Both these methods are similar but not equivalent. The first adds interpolated fields to the model fields the second scales the existing model field in a spatially varying manner.

$$M_{OK\_NRES}(x, y) = \left[ \sum_{i=1}^n \lambda_i \frac{O(x_i, y_i)}{M(x_i, y_i)} \right] \times M(x, y)$$

One of the major problems with kriging of the residual is that the semi-variogram is less well defined since much of the covariance is removed in the subtraction of the trend. Since it is often poorly defined the semi-variogram parameters can be determined by minimising the cross validation RMSE.

### 3.4.4 Bayesian assimilation of kriged and model fields

There is a tendency in kriging methods, which are based on observations, to treat the observed quantities as being error free. Kriging itself is an exact interpolator in as much that the weighting of  $\lambda_i$

at the position  $(x_i, y_i)$  will necessarily be 1 in order to minimise the variance at that point. However, when large nugget:sill ratios are present in the semi-variogram this effect is only present at exactly the same point in space as the observation and will lead to gridded maps that deviate from the observed value at the nearest grid square. In reality there are uncertainties attached to the observations, as well as the model, and data assimilation methods based on Bayesian statistics, such as OI and variational methods, take into account these uncertainties when combining observations and models.

The method applied here is similar to these methods in nature but simpler in implementation. It assumes a known uncertainty for the model field, at all points in space, and a known uncertainty in the observational field, at all points in space. The observational field is described by the ordinary kriging interpolation field. The uncertainty of that field is described by the variance, which is calculated at every point of the kriging interpolation. The model field uncertainty is given by the RMSE of the model field, calculated by comparison with the observations (see section 3.5.3).

If the uncertainty is assumed to be Gaussian in nature, ie. the probability density function (PDF) is Gaussian and unbiased, then an assimilated field can be produced by combining the observational and model field in a straightforward manner.

$$M_{BA}(x, y) = \frac{\sigma_o^2 M(x, y) + \sigma_M^2 O(x, y)}{\sigma_o^2 + \sigma_M^2}$$

where  $\sigma$  is the standard deviation at that point in space of the model ( $M$ ) and observational ( $O$ ) field. The resulting uncertainty, in terms of standard deviation of the assimilated field will be given by

$$\sigma_{BA}^2(x, y) = \frac{\sigma_o^2 \sigma_M^2}{\sigma_o^2 + \sigma_M^2}$$

The assimilated concentration field will then be a weighted combination of the observed and modelled field, the weight given to the assimilated values being dependent on the relative uncertainties of the observed and modelled fields. In areas far from observations the resulting field will be equivalent to the model field since the observational field uncertainty is much larger than the modelled field uncertainty. In areas close to observations the fields will approach the observations but still be dependent on the relative uncertainty of the kriged and modelled field.

Due to the Gaussian assumption used here application of this method is most appropriate when the model field is unbiased, i.e the expectance value of the PDF is the same as the value of the concentration. Correcting for the bias should be carried out before application of this method and this is achieved to a large extent by using linear regression, described in section 3.4.1

### 3.5 Uncertainty mapping

A number of methods can be considered when mapping the uncertainty, dependent on the method used to produce the map and on the parameter that should be shown. In this study methods for presenting uncertainty of particular parameters will be explored.

#### 3.5.1 RME as an uncertainty parameter

The Relative Maximum Error (RME) is presented in the EU daughter directives (EC, 1999; EC, 2002) as an uncertainty indicator that should be applied to assess model quality. When applied to annual means this indicator is almost the same as the absolute relative bias of a model in regard to observations. It is defined by

$$RME_i = \left| \frac{M_i - O_i}{O_i} \right|$$

This parameter can only be determined at points in space corresponding to observations. The directives give various recommended values that this parameter should not exceed. For annual means this is 50% for PM<sub>10</sub> and 30% for NO<sub>2</sub> and SO<sub>2</sub>.

### 3.5.2 Spatial interpolation of RME

Since this parameter is only assessed at points in space it can be presented in its simplest form as dots on a map indicating, through colouring or dot size, its value. It is of course possible to interpolate this value, using for example kriging methods, in space but the interpolation brings with it its own uncertainty and it is not useful to introduce the uncertainty of uncertainty in a quantity. For this reason any spatial representation of the RME should be limited, based on the spatial variance of the parameter. This means for instance that if kriging is used to interpolate RME that only regions with high interpolation certainty should be shown, based on the interpolation variance calculated in kriging.

### 3.5.3 Indicative RMSE

An uncertainty map can be produced by calculating the root mean square error (RMSE) of the model based on the available observations.

$$RMSE = \sqrt{\frac{1}{n} \sum_{i=1}^n (M_i - O_i)^2}$$

By normalising this with the mean of the modelled, or observed, concentrations at the observational points the normalised RMSE (NRMSE) can be determined

$$NRMSE = \frac{RMSE}{\bar{M}_i}$$

If this is assumed to be representative of the typical relative error of the model then this can then be multiplied with the model field to produce an uncertainty map giving absolute values. The difference between the NRMSE and the average normalised absolute bias (ANB), another measure of uncertainty that for annual mean values is equivalent to the average RME, is that the former is squared and as such weighted towards the larger differences. RMSE is more closely related to quantities such as standard deviation (SD), which can also be used in assessment. In fact, when regression is used, i.e, there is no bias in the model, then the RMSE is equivalent to the SD of the regression model.

Normalising with the model concentrations is carried out when estimating the field uncertainties but for assessment purposes the RMSE is always normalised with the observational mean to provide consistency with varying model results.

There are also other methods, when using regression analysis, to estimate the 'confidence' or 'prediction' interval of the regression. Such methods have been discussed in the London case study (Air4EU – CS D7.1.10) and use student-t distributions when the number of observations is small. If the number of observations is larger then it is also possible to calculate, for example, the standard deviation of the residual as a function of model concentration, in order to assess more clearly how the uncertainty varies with concentration. In this case study we limit ourselves to the use of the RMSE as an indicator of relative uncertainty.

### 3.5.4 Kriging and assimilation uncertainty fields

The uncertainty in the kriged fields, be they derived from kriging or residual kriging, can be shown using the kriged variance calculated at each interpolated point. This variance is interpreted to be equivalent to the square of the standard deviation and is based on the form of the semi-variogram. The nature of the semi-variogram, that of increasing variance with distance from observations, means that uncertainty maps based on kriging will show lowest uncertainties around the observations, increasing to the sill value far from the observations.

Similarly, the Bayesian assimilated fields, based on model and observational field uncertainties, can also be shown spatially as a map. These will resemble the model uncertainty fields but with, generally, decreased uncertainty near observational points.

### 3.5.5 Cross validation of the observational mean and the RMSE

As previously described, cross validation and its RMSE is used throughout this case study to assess the quality of the assimilation methods. From a statistical perspective the following note is made:

The simplest 'model' that can be used to describe the concentration field is simply the mean of all the observations. Taking the RMSE of this 'model' is equivalent to calculating the standard deviation (SD) of the observations. Any assimilated field should be able to improve on the observational SD as a method for estimating the concentration field.

Since there are limited observations available cross validation, similar to the jack knife method used for estimating uncertainty in a limited sample set, is also used to assess this quantity. This will be larger than the observational SD but for large n will necessarily approach it.

## 3.6 Probability of exceedance maps

Given both concentration and uncertainty fields it is also possible to determine the probability of exceedance (POE), given some limit value (LV). This is done by integration of the probability density function (PDF). If the PDF is Gaussian such that the normalised PDF can be written:

$$PDF = \frac{1}{\sqrt{2\pi}\sigma} \exp\left(-\frac{(c - c_0)^2}{2\sigma^2}\right)$$

where  $c_0$  is the expectance value and  $\sigma$  is the variance. The POE can then be written as follows:

$$POE = \int_{LV}^{\infty} PDF dc = \frac{1}{2} \operatorname{erfc}\left(\frac{(LV - c_0)}{\sqrt{2}\sigma}\right)$$

where  $\operatorname{erfc}$  is the complimentary error function. The POE will always be 50% when  $LV = c_0$  but will increase, or decrease, dependent on the variance. At the point where  $LV = c_0 \pm \sigma$  then  $POE = 50\% \pm 35\%$ . At this point there is thus 85% probability that there is, or is not, an exceedance. This is demonstrated in figure 3.3 below.

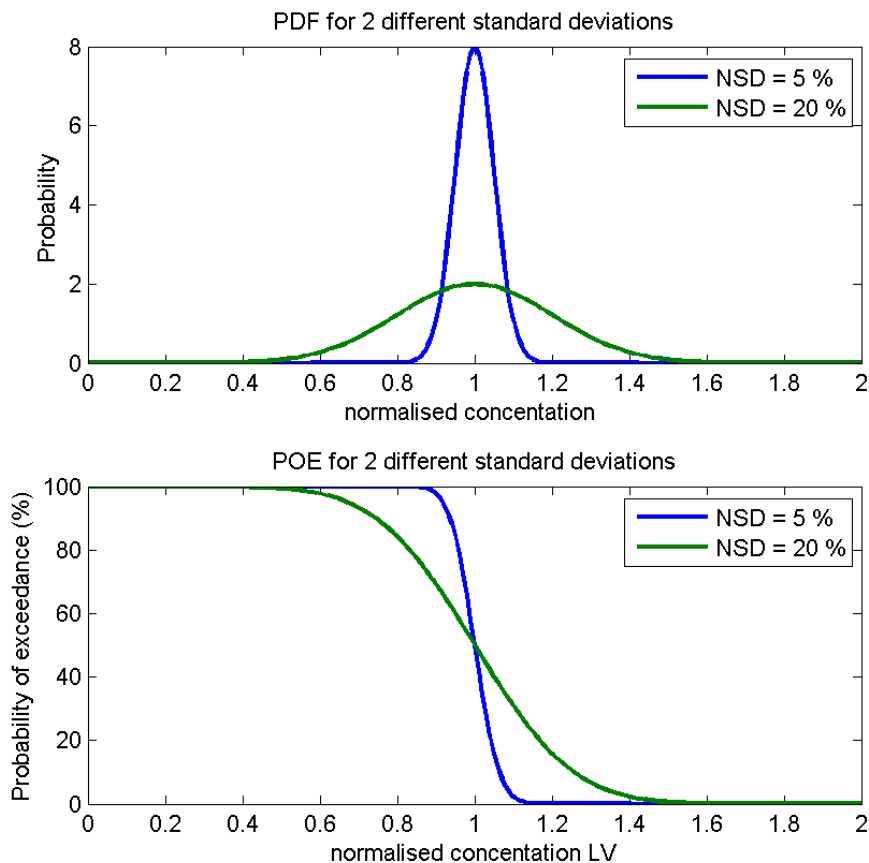


Figure 3.3: The Gaussian probability density function (PDF) top and the corresponding probability of exceedance (POE) bottom for a normalised concentration and 2 different normalised standard deviations (NSD).

## 4. Results

In this section the results of the various assimilation methods are described. These are chiefly shown as tables in the bulk of the text. In section 4.8 a selection of the concentration and uncertainty maps are presented for the 3 different pollutants PM<sub>10</sub>, SO<sub>2</sub> and NO<sub>2</sub>. Discussion concerning the results and methods will be addressed in section 5.

### 4.1 Statistical analysis of model and observations

The following table provides basic statistics for the modelled and observed annual mean concentrations.

Table 4.1: Basic statistical parameters of the yearly average modelled and observed concentrations at the 12 observational sites. Model parameters provided are for the grids corresponding to the observational positions with the exception of the 'Total model' parameters that include all the grid values. (\* Indicates estimates of the model background value but these have not been assessed)

Parameter	Annual mean PM <sub>10</sub>		Annual mean SO <sub>2</sub>		Annual mean NO <sub>2</sub>	
	Obs	Mod	Obs	Mod	Obs	Mod
Mean (ug/m <sup>3</sup> )	44.0	38.0	7.9	7.3	40.4	31.2
Max (ug/m <sup>3</sup> )	58.6	49.0	10.5	9.4	50.1	43.8
Min (ug/m <sup>3</sup> )	35.7	32.7	6.4	4.4	28.7	18.3
SD (ug/m <sup>3</sup> )	5.4	4.7	1.0	1.6	7.1	7.9
Total model max (ug/m <sup>3</sup> )		69.3		12.6		85.1
Total model min (ug/m <sup>3</sup> )		18.1		3.5		12.4
Regional BG (ug/m <sup>3</sup> )	26.3	5*	4.0	7*	11.9	5*
RMSE (ug/m <sup>3</sup> )	7.3		1.3		11.1	
NRMSE (%)	16.6 %		16.7 %		27.4 %	
Mean RME (%)	14.1 %		15.0 %		23.1 %	
CV RMSE Mean obs (ug/m <sup>3</sup> )	5.9		1.13		7.8	

From the above it is interesting to compare the RMSE of the modelled concentrations with the CV RMSE of the mean observations (slightly larger than the observed SD). From a statistical perspective this value, for all three of the compounds, is smaller than the modelled RMSE. This indicates that on a statistical basis simply taking the mean of the observations would give a better RMSE than the model currently gives. However, the correlation will likely be much worse. This is pointed out here because improvement through assimilation of the observations into the model will be assessed through the cross validation RMSE and for any improvement to be considered significant then it must produce an RMSE that is lower than the observed SD.

## 4.2 Linear regression

A linear regression relationship between modelled and observed data can be determined in a number of ways. Here 3 separate methods are applied. These are:

1. Linear regression model where  $M_{LR1} = a_1 + b_1M$
2. Linear regression with 0 intercept and subtraction of model and observed background values such that  $M_{LR2} = b_2(M - M_{BG}) + O_{BG}$
3. Linear regression with slope = 1 but with varying intercept  $M_{LR3} = a_3 + M$

In principle the first method should be applied as it is the most general. The calculated linear fit should indicate the background value that best minimises the RMSE for the regression as well as providing a slope for multiplication. However, when correlation is poor the slope may be very uncertain and should not be used to determine the background value. Method 2 address this by taking assumed background values, from both model and observations, and fitting a linear regression that is forced to pass through this point. The model and observed background values may differ, as in the ATEM case (See table 4.1) and there is some uncertainty to their actual value. Method 3 is also a special case where only the background value is allowed to vary and the slope is not adjusted. This is equivalent to subtracting the mean bias of the model receptor points. This last method is appropriate when background levels are not well known and the range of available values is limited.

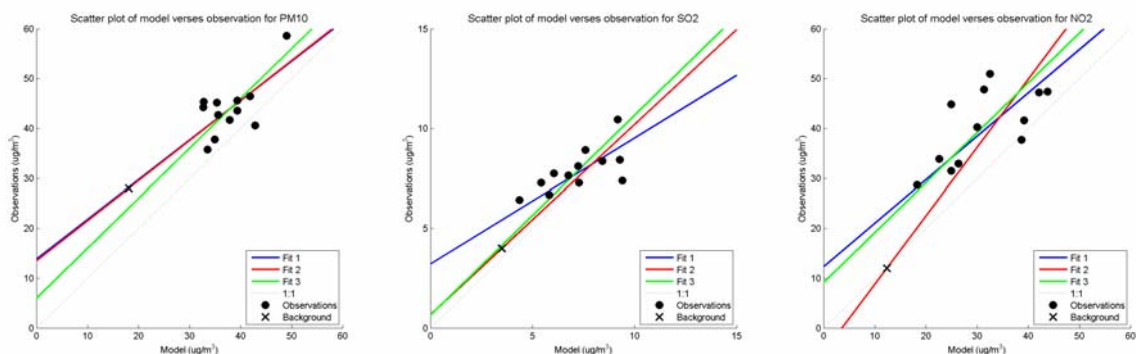


Figure 4.1: Scatter plots of annual mean observations and corresponding ATEM model grid values for the three pollutants  $PM_{10}$ ,  $SO_2$  and  $NO_2$  (black circles). Included are the estimated background concentrations (black cross). The 3 different regression plots, described in the text, are shown: 1. Linear regression (blue); 2. subtracted background (red) and 3. subtraction of bias (green).

For the current application rural background values for the ATEM model are calculated based on input from another numerical model and on point sources outside of the model region (Brechler, 2000). This particular model is known to underestimate  $PM_{10}$  levels. Observed background values for the 3 components can be estimated from rural background stations in the vicinity of Prague and are listed in table 4.1. However, there can still be a sizable uncertainty in these values. In the case of  $SO_2$  for instance the rural background at some nearby stations is larger than a number of the Prague stations and so its value must be treated with caution. Due to uncertainty in the model background values the model background is taken to be the minimum model field value in the above regressions.

Table 4.2: Results of the regression analysis showing slope, y intercept, correlation coefficient and the RMSE and NRMSE, using all observations and also using cross validation (in square brackets).

Annual mean $PM_{10}$ regression analysis			
Method	Fit 1	Fit 2	Fit 3
Slope	0.79	0.8	1.0
Y intercept ( $ug/m^3$ )	13.85	13.5	6.0
$R^2$	0.67	0.45	0.45
RMSE [CV] ( $ug/m^3$ )	4.01 [5.81]	4.01 [4.45]	4.14 [4.51]
NRMSE [CV] (%)	9.1 [13.2]	9.1 [10.1]	9.4 [10.3]

Annual mean $SO_2$ regression analysis			
Method	Fit 1	Fit 2	Fit 3
Slope	0.63	0.95	1.0
Y intercept ( $ug/m^3$ )	3.21	0.67	0.65
$R^2$	0.62	0.46	0.46
RMSE [CV] ( $ug/m^3$ )	0.82 [0.95]	1.14 [1.28]	1.15 [1.25]
NRMSE [CV] (%)	10.4 [12.1]	14.8 [16.2]	14.5 [15.9]

Annual mean $NO_2$ regression analysis			
Method	Fit 1	Fit 2	Fit 3
Slope	0.87	1.37	1.0
Y intercept ( $ug/m^3$ )	12.3	-5.0	9.14
$R^2$	0.60	0.43	0.43
RMSE [CV] ( $ug/m^3$ )	5.88 [6.19]	8.55 [9.32]	6.27 [6.84]
NRMSE [CV] (%)	14.6 [15.3]	21.2 [23.1]	15.5 [16.9]

The results shown in figure 4.1 and table 4.2 indicate that the 3 different fitting methods can give quite similar as well as differing results. They also vary in their sensitivity to the cross validation exercise. Which of the 3 fitting methods should be applied is dependent on the confidence in the results. The PM<sub>10</sub> linear fit, for example, is strongly affected by a single large value and there is low confidence in the resulting fit since the cross validation RMSE is significantly higher than the RMSE.

For SO<sub>2</sub> there is less confidence in the observed background value and for NO<sub>2</sub> the fit is significantly good to warrant confidence in the linear regression. However, as a basic principle it is recommended to subtract the background values and use the second type of fitting if the background concentrations are well established, even though this will not minimise the RMSE.

The regression model fit leads to significant improvements in the RMSE for both PM<sub>10</sub> and NO<sub>2</sub>, though less significant for SO<sub>2</sub>. The RMSE values are generally lower than the observed mean CV RMSE which indicates improvement beyond the simple observational mean model, see section 4.1. For further analysis, visualisation and residual kriging, fit 2 will be applied for PM<sub>10</sub> whilst fit 1 will be applied for SO<sub>2</sub> and NO<sub>2</sub> since these give the lowest CV RMSE.

The resulting maps are shown in figures 4.6c – 4.8c.

### 4.3 Kriging of observations

Observational fields can be created by kriging the observed values. Kriging is a statistical method that relies heavily on the defined semi-variogram form. The semi-variogram represents the variance as a function of distance, or lag, from any point in the field. Generally the definition of the semi-variogram should be based on the empirically determined variance but since the number of observations is low in the Prague case the empirically determined variance is not expected to give a clear definition of the actual spatial variance. 3 different methods can thus be applied to determine the parameters of the semi-variogram. These are:

1. Best fit to the observed spatial variance
2. Best fit to the model field spatial variance
3. Use the parameters that minimise the cross-validation RMSE

The empirical semi-variograms for 1 and 2 above are shown in figures 4.2 and 4.3 below along with estimated fits to their values. As can be seen in figure 4.2 the semi-variograms are not well defined for the observations. For the model fields however there is a clear correlation between distance and variance up to around 10 km which is the representative scale of the concentration features in the fields.

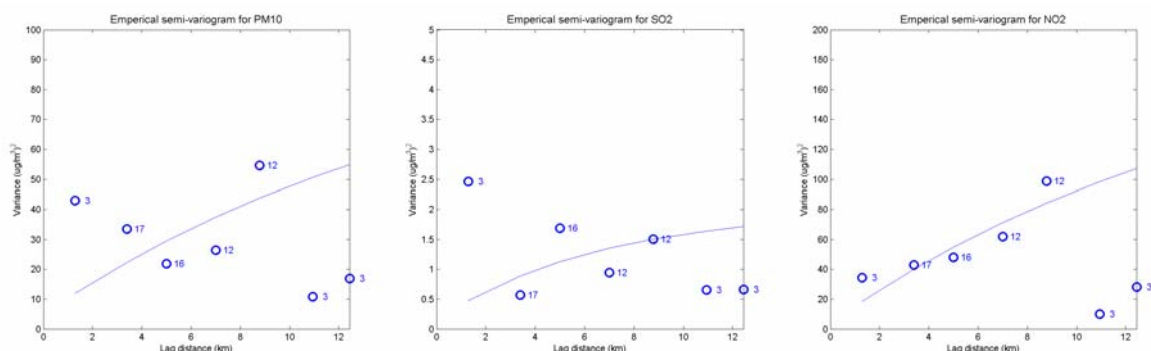


Figure 4.2: Empirical semi-variograms (circles) and exponential model fit (solid line) based on the observations. Parameters for the fit are given in table 4.3. Left  $PM_{10}$ , middle  $SO_2$  and right  $NO_2$

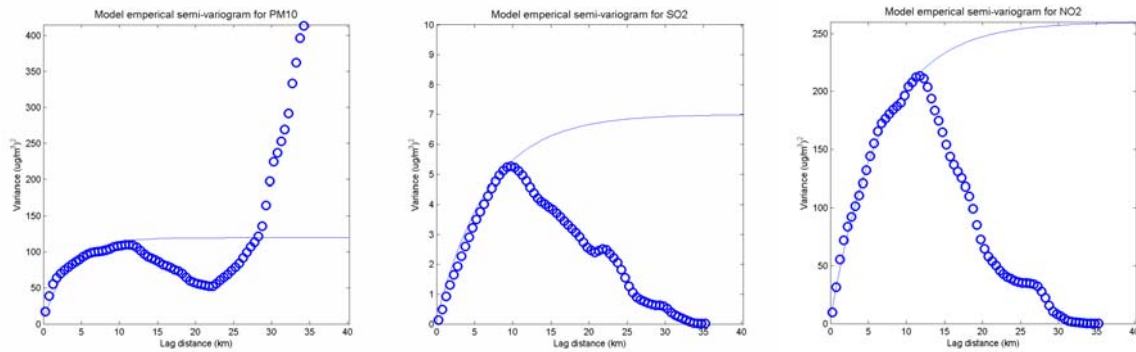


Figure 4.3: Empirical semi-variograms (circles) and exponential model fit (solid line) based on the ATEM model. Parameters for the fit are given in table 4.3. Left  $PM_{10}$ , middle  $SO_2$  and right  $NO_2$

There are some points in regard to the semi-variograms that need to be included in choosing any semi-variogram model. Firstly the sill value obtained from the observational variance is not expected to be as well represented as that for the model variance simply because the stations are positioned in similarly polluted areas and there are far fewer observations available than there are model grid squares. It is therefore recommended in this case to adopt a sill value based on the model variance. Though the value of the sill is not important for determination of the kriging weights it is important when uncertainty estimates are being made. Secondly the range of the semi-variogram is expected, based on the model, to lie in the region of around 10 km. Ranges larger than 20 km would seem unrealistic for the variance function considering the spatial variations of emissions. Thirdly the cross validation RMSE will always be least for method 3 but, as seen above, the values, e.g. range, could be quite unrealistic. Fourthly, we require the nugget value to be representative of the expected observational uncertainty, including its spatial representativeness This is estimated at 5% of the mean observed value for the current application.

Table 4.3: Semi-variogram model parameters determined using the 3 different methods outlined in the text. The column labelled 'Applied' lists the parameters used in the Bayesian assimilation. These are slightly different to the other parameters as the nugget:sill ratio is adjusted to represent observational uncertainty.

Annual mean $PM_{10}$ ordinary kriging analysis				
Method	1	2	3	Applied
Variogram model	Exp.	Exp.	Sphere.	Sphere.
Range (km)	50	10	9.5	10
Sill ( $ug/m^3$ ) <sup>2</sup>	60	120	120	120
Nugget:sill ratio	0.08	0.04	0.5	0.12
RMSE CV ( $ug/m^3$ )	6.05	6.12	5.7	6.02
NRMSE CV (%)	13.8%	14.0%	13.0%	13.7%

Annual mean $SO_2$ ordinary kriging analysis				
Method	1	2	3	Applied
Variogram model	Exp.	Exp.	Sphere.	Sphere.
Range (km)	20	20	11	10

Sill ( $\mu\text{g}/\text{m}^3$ ) <sup>2</sup>	1.2	7.0	7.0	7
Nugget:sill ratio	.13	.02	0.25	0.02
RMSE ( $\mu\text{g}/\text{m}^3$ )	0.98	1.02	0.94	1.02
NRMSE (%)	12.5%	13.0%	12.0%	12.8%

Annual mean NO <sub>2</sub> ordinary kriging analysis				
Method	1	2	3	Applied
Variogram model	Exp.	Exp.	Sphere.	Sphere.
Range (km)	50	20	10.5	10
Sill ( $\mu\text{g}/\text{m}^3$ ) <sup>2</sup>	160	260	260	260
Nugget:Sill ratio	0.02	0.03	0.10	0.02
RMSE ( $\mu\text{g}/\text{m}^3$ )	6.95	7.03	6.21	6.33
NRMSE (%)	17.2%	17.4%	15.3%	15.6%

Based on these conditions and the need to introduce some form of consistency in regard to the range, the parameters listed in tables as 'applied' were adopted for the further kriging interpolation even though they were not optimal in regard to minimising the CV RMSE. The resulting maps are shown in figures 4.6b – 4.8b.

#### 4.4 Kriging of the observed – modelled residual

Since kriging assumes spatial homogeneity a method also applied to generate fields is to subtract the model concentrations from the observed values. This produces a set of residuals that can be spatially interpolated to improve the spatial maps created. 4 different methods are applied as follows:

1. Residual of observations - model
2. Normalised residual of the observations - model
3. Residual of observations - regression model
4. Normalised residual of the observations - regression model

The form of these 4 methods is described in section 3.4.3

One of the major obstacles to applying this method is that finding a useful semi-variogram is difficult. Examples of the 3 empirical variograms for the observed – model residuals are shown below in figures 4.4. Only for PM<sub>10</sub> is there any indication of a positive functional relationship between variance and lag distance.

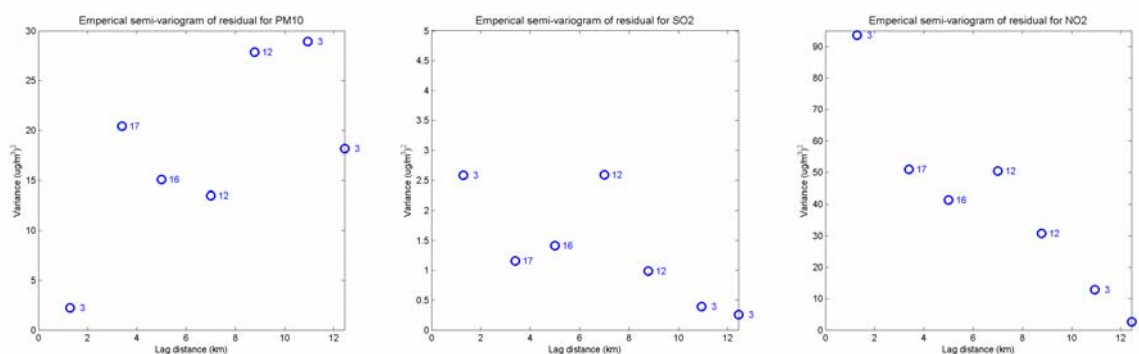


Figure 4.4: Empirical semi-variograms (circles) based on the residual of observations - model. Left PM<sub>10</sub>, middle SO<sub>2</sub> and right NO<sub>2</sub>

As a result the range and nugget:sill ratio are determined for the residual kriging by minimising the cross validation RMSE. The results, for the 4 different interpolation methods outlined above are given in table 4.4. In general kriging of the residual, be it for the model or the regression model, does not improve the results. With the exception of SO<sub>2</sub> the minimising variograms lead to an almost pure nugget variogram. Such a variogram simply interpolates the regional mean, which can equally well be removed by using one of the linear regression methods. The inference of this is that there is no spatial correlation in the residual field structure and so kriging is not an effective spatial interpolator under such conditions.

*Table 4.4: Semi-variogram model parameters determined for the 4 different residual methods outlined in the text. The parameters are determined based on minimisation of the cross validation RMSE.*

	Mean PM <sub>10</sub>			
Method	1	2	3	4
Range (km)	1.5	1.5	1.5	1.5
Sill (ug/m <sup>3</sup> ) <sup>2</sup>	12.0	12.0	12.0	12.0
Nugget:Sill ratio	0.0	0.0	0	1.0
RMSE (ug/m <sup>3</sup> )	4.49	4.79	4.41	4.39
NRMSE (%)	10.2%	10.9%	10.1%	10.0%

	Mean SO <sub>2</sub>			
Method	1	2	3	4
Range (km)	8	8	29.5	30
Sill (ug/m <sup>3</sup> ) <sup>2</sup>	2.5	2.5	2.5	2.5
Nugget:Sill ratio	0.65	0.5	0.65	0.6
RMSE (ug/m <sup>3</sup> )	1.19	1.29	0.94	0.94
NRMSE (%)	15.1%	16.4%	12.0%	12.0%

	Mean NO <sub>2</sub>			
Method	1	2	3	4
Range (km)	0.5	0.5	1.5	1.5
Sill (ug/m <sup>3</sup> ) <sup>2</sup>	38	38	38	38
Nugget:Sill ratio	0.0	0.0	0.60	0.75
RMSE (ug/m <sup>3</sup> )	6.84	8.81	6.19	6.18
NRMSE (%)	16.9%	21.8%	15.3%	15.3%

Methods 3 and 4 above are built on the ‘best’ regression method applied in section 4.2.

#### 4.5 Bayesian combination of the observed and modelled fields

The observational field determined using kriging and its error variance field, section 4.3, can be combined with the model or model regression field using Bayesian statistics. The method by which this is achieved is described in section 4.1. The result will be very similar to that from optimal interpolation when the covariance matrix is defined by the same distance dependent structure as used in kriging. The result will differ from the previous section on residual kriging as it will also depend on the relative uncertainty of the two fields. In the residual method applied in section 4.4 no regard was taken for model uncertainty when adding the model to the interpolated residual.

Table 4.5 below provides the cross validation results of the assimilation for both the model and the regression model fields. The resulting maps are shown in figures 4.6d – 4.8d.

Table 4.5: Cross validation RMSE for the Bayesian assimilation method used with both the model and the regression model fields

Results of the Bayesian assimilation			
Pollutant	PM <sub>10</sub>	SO <sub>2</sub>	NO <sub>2</sub>
CV RMSE – model (ug/m <sup>3</sup> )	5.85	1.23	7.75
CV NRMSE – model (%)	13.3 %	15.6 %	19.2 %
CV RMSE – regression (ug/m <sup>3</sup> )	4.48	0.96	6.03
CV NRMSE – regression (%)	10.2 %	12.2 %	14.9 %

In regard to assimilation of the kriged and model fields the results show CV RMSEs that are improved in regard to the model fields (table 4.1) but do not improve on the kriged fields. This is due, to a large extent, on the bias in the model field, which is removed through the regression. When the regression model field is used for the assimilation then very similar CV RMSEs are obtained to the other methods of regression and residual kriging (tables 4.3 and 4.4).

#### 4.6 Summary of the assimilation methods

To compare the results of the cross validation assessment of the assimilation methods applied in the previous sections figure 4.5 displays the NRMSE of the methods for all 3 pollutants. In this figure all the results shown are based on cross validation. The results are compared, dotted horizontal line, to the simplest case where the CV RMSE of the observational mean is determined. Any useful assimilation method, analysed statistically, should improve on this. That the model RMSE is larger than this indicates that statistically significant improvement is possible. Improvement below this level is achieved using all assimilation methods. As was shown in section 4.2 simply removing the bias of the model can significantly improve the RMSE.

In figure 4.5 the regression RMSE shown is the 'best' according to table 4.2. For PM<sub>10</sub>, SO<sub>2</sub> and NO<sub>2</sub> these are methods 2, 1 and 1 respectively. Direct interpolation by kriging of the observations should improve upon the mean observational RMSE, which it does in all cases. The improvement is dependent on the spatial correlation of the observations. This point is evident in the residual kriging where there is little or no spatial correlation in the residual, leading to almost pure nugget variograms. There is very little improvement in the RMSE as a result of residual kriging in this case. More improvement would be apparent if the residual was better spatially correlated. Finally the Bayesian combination of kriged and regression model RMSE is also included. This method gives very similar RMSE to the other assimilation techniques when the observational field is combined with the regression model. For the case of NO<sub>2</sub> this actually provides the 'best' result.

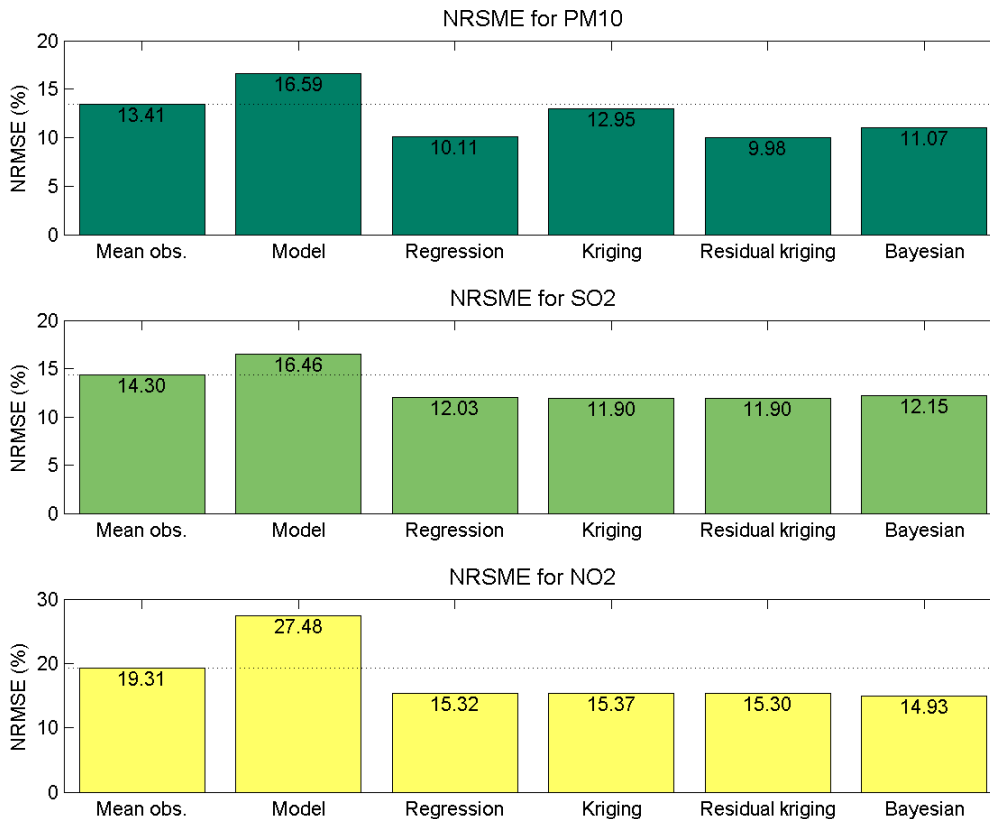


Figure 4.5: Summary of the cross validation RMSE of the assimilation methods tested showing the NRMSE, normalised with the mean of the observations, as %. The thin horizontal line corresponds to the cross validated mean observational standard deviation. Top PM<sub>10</sub>, middle SO<sub>2</sub> and bottom NO<sub>2</sub>

#### 4.7 Final set of concentration and uncertainty maps

In order to intercompare the various results discussed in the previous sections the pollutant and calculated uncertainty maps are displayed here for the 3 components PM<sub>10</sub>, SO<sub>2</sub> and NO<sub>2</sub>. Four sets of maps are shown, those being:

- The original model map with uncertainty based on the normalised RMSE multiplied by the model concentration.
- The observational kriged map with uncertainty based on the kriging variance.
- The 'best' regression map with uncertainty based on the normalised CV RMSE multiplied by the model regression concentration.
- The Bayesian assimilated map, based on the combination of the observational kriged map and the 'best' regression model, with uncertainty calculated from the combined maps.

Clearly the observational kriged maps are of the poorest quality, particularly far from the observations. The uncertainty in the regression maps is significantly less than the original model map and the use of Bayesian assimilation improves the uncertainty of the maps, particularly in the areas where observations are available.

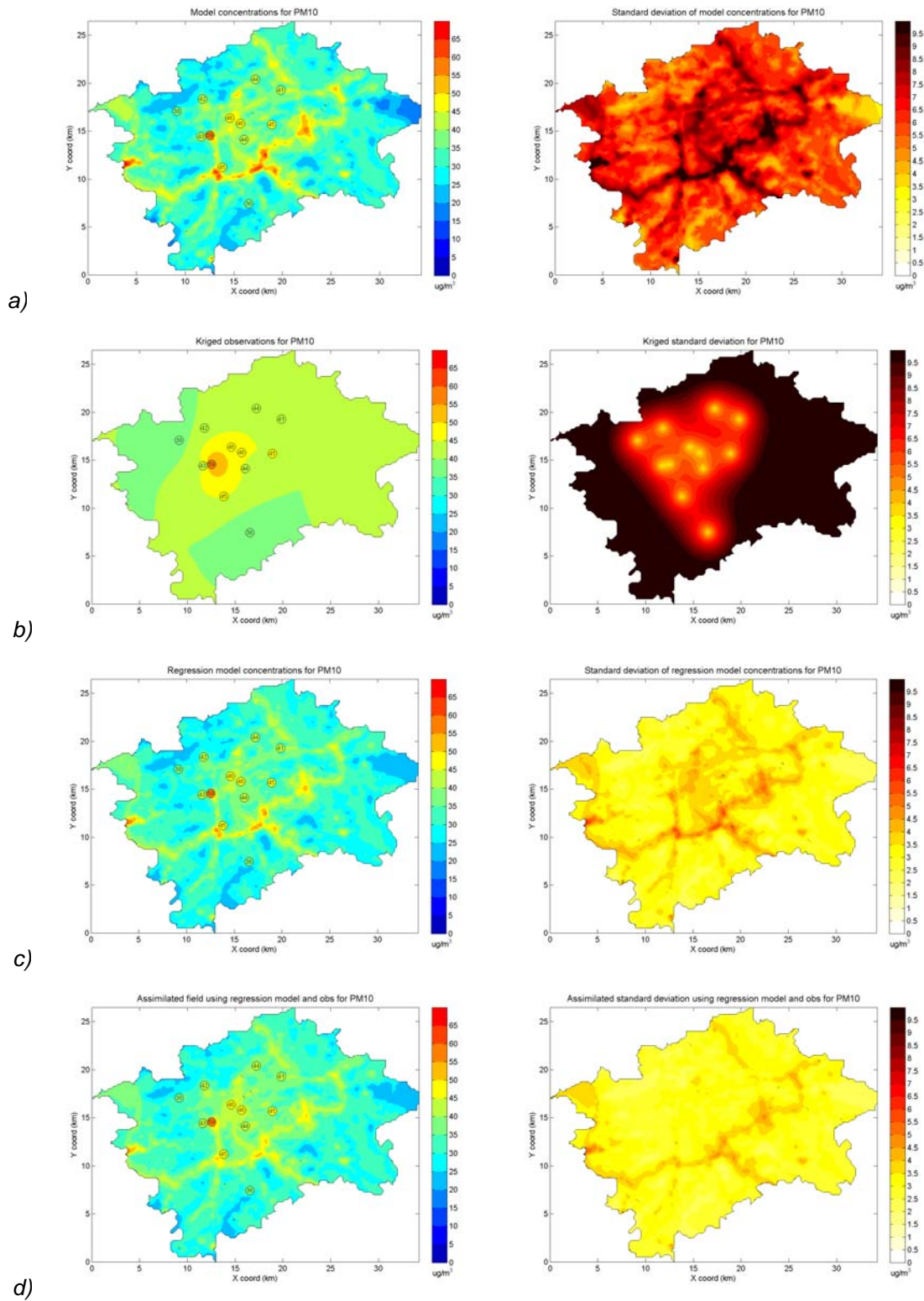


Figure 4.6: Final set of annual mean concentration maps (left) and uncertainty maps (right) for PM<sub>10</sub>. a) Model field, b) Kriged field, c) Model regression field and d) Bayesian combined field. See text for more details.

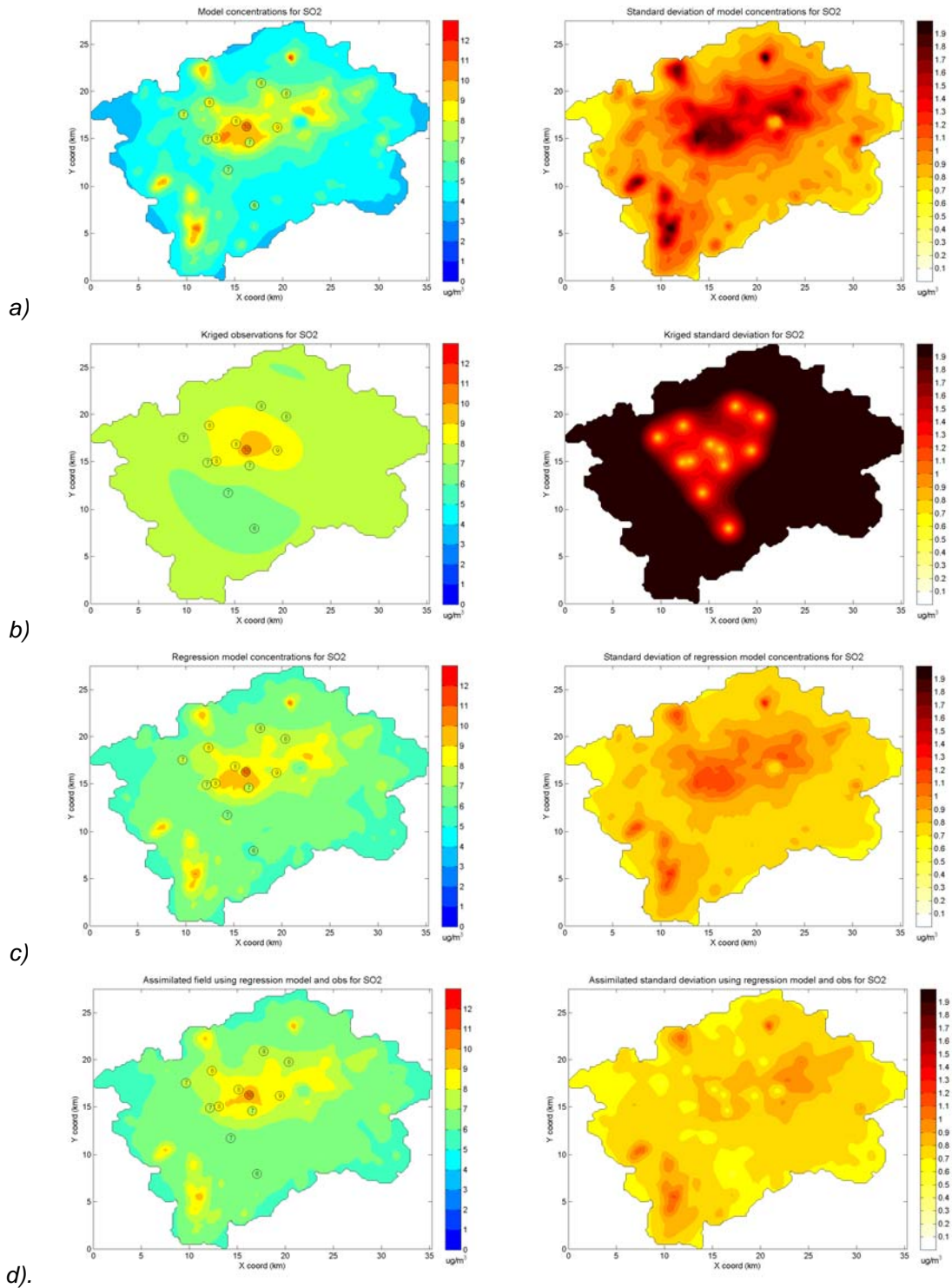


Figure 4.7: Final set of annual mean concentration maps (left) and uncertainty maps (right) for SO<sub>2</sub>. a) Model field, b) Kriged field, c) Model regression field and d) Bayesian combined field. See text for more details.

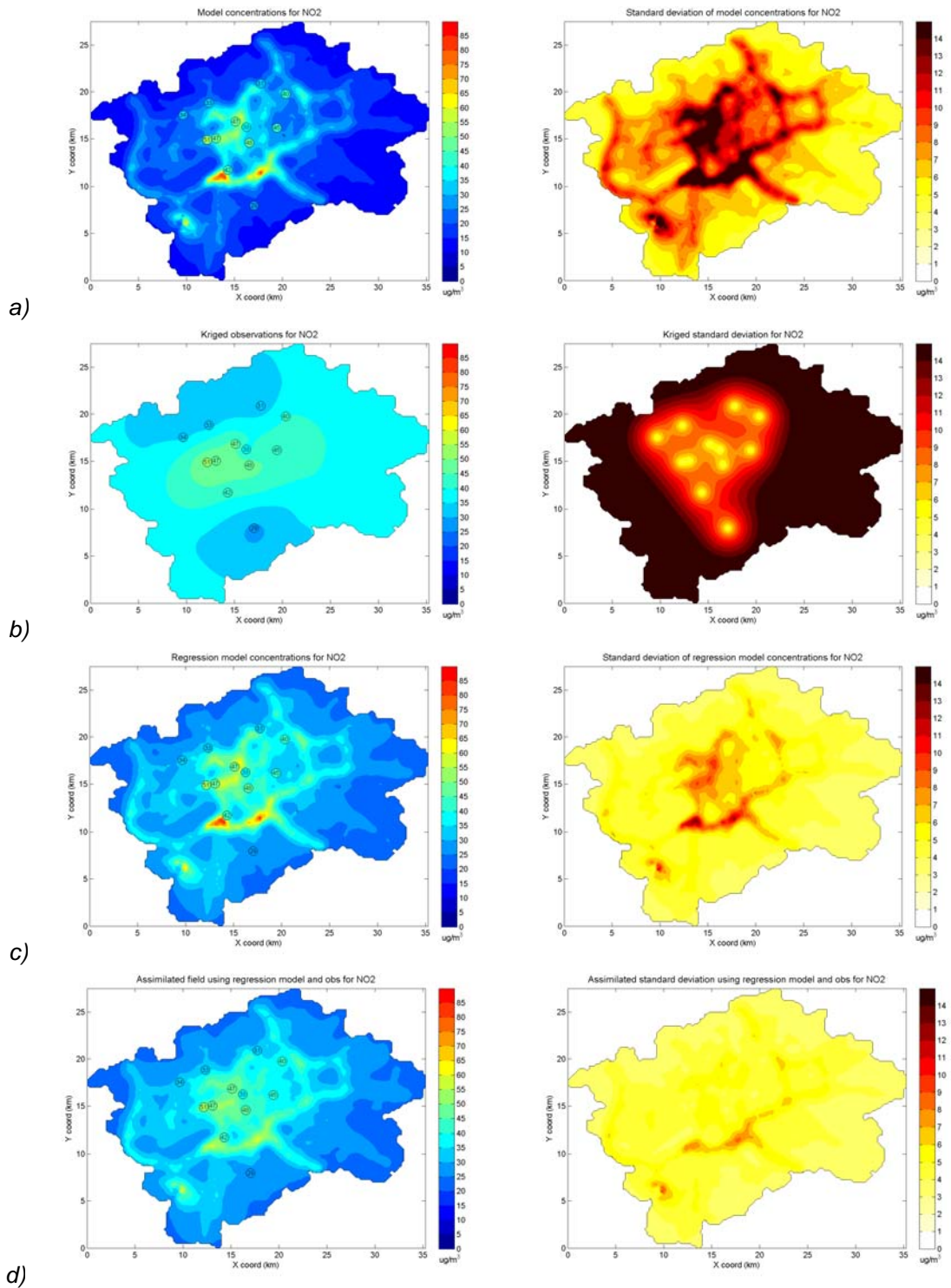


Figure 4.8: Final set of annual mean concentration maps (left) and uncertainty maps (right) for NO<sub>2</sub>. a) Model field, b) Kriged field, c) Model regression field and d) Bayesian combined field. See text for more details.

## 4.8 Mapping of RME as an uncertainty indicator

The relative maximum error (RME) is a model error assessment applied in the EU Daughter directives and so is examined in more detail here, see section 3.5.1 for a definition. The question addressed here is whether such an indicator can also be mapped. Two methods were tested.

1. Regression analysis with model concentrations
2. Spatial interpolation of RME using kriging

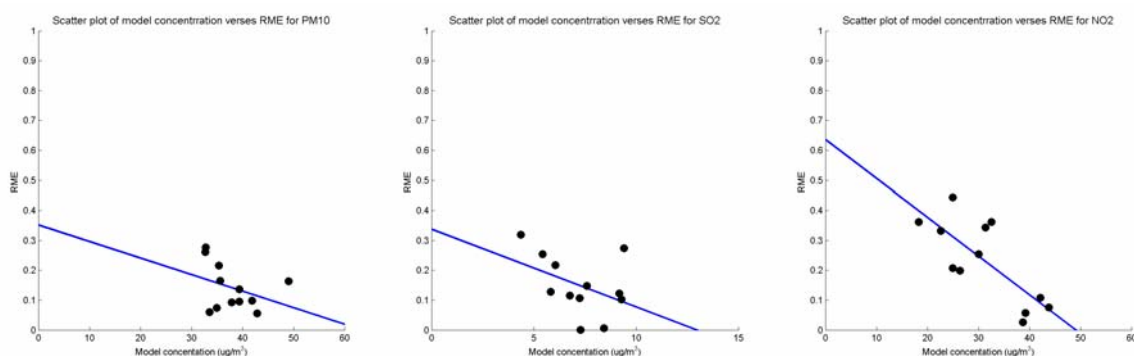


Figure 4.9: Scatter plots of annual mean RME and corresponding ATEM model grid concentrations for the three pollutants  $PM_{10}$ ,  $SO_2$  and  $NO_2$  (black circles). The linear regression plot is also shown.

Table 4.6: Results of the regression analysis for RME showing slope, y intercept and correlation coefficient.

RME regression analysis			
Pollutant	$PM_{10}$	$SO_2$	$NO_2$
Slope	-0.0055	-0.0261	-0.0130
Y intercept ( $\mu g/m^3$ )	0.35	0.34	0.64
$R^2$	0.12	0.18	0.58

From figure 4.9 and table 4.6 it can be seen that, with the exception of  $NO_2$ , there is very little correlation between RME and model field concentrations. However all three compounds indicate decreasing RME with increasing concentrations and the high correlation for  $NO_2$  indicates that the model RME can be related to the actual model concentrations. This in fact reflects model bias. If the model is consistently biased (in absolute terms) then a clear correlation of RME against model concentration will be found. A consistent model bias can be most clearly seen for  $NO_2$ , figure 4.1, and this is reflected in the RME correlation given in table 4.6. It thus may be indicative to map RME using linear regression when the model bias is well defined, but this can lead to problems when the linear regression provides negative values for RME. As a result it is not recommended to use regression of this type, though other functional forms may be better suited for the regression.

In a similar fashion kriging may also be applied to try to interpolate the RME in a meaningful way spatially. This was carried out in a similar fashion to the residual kriging in that the semi-variogram parameters were adjusted to obtain the minimum RMSE. The results, not shown here, are similar to the residual kriging in that the best fit to the semi-variogram parameters is a pure nugget form. This means that the RMSE was minimised by creating a field that was simply the mean of the observed RME. Kriging is thus not a useful method for spatial interpolation of RME in this case since there is very low spatial correlation of this parameter. This follows from the same result obtained from residual kriging

In conclusion, neither regression nor kriging is a useful, or robust, method for spatial interpolation of the RME for the case at hand. The RME should thus only be shown at the individual observational points and not interpolated in space. Such a representation is shown for the 3 compounds below in figure 4.10.

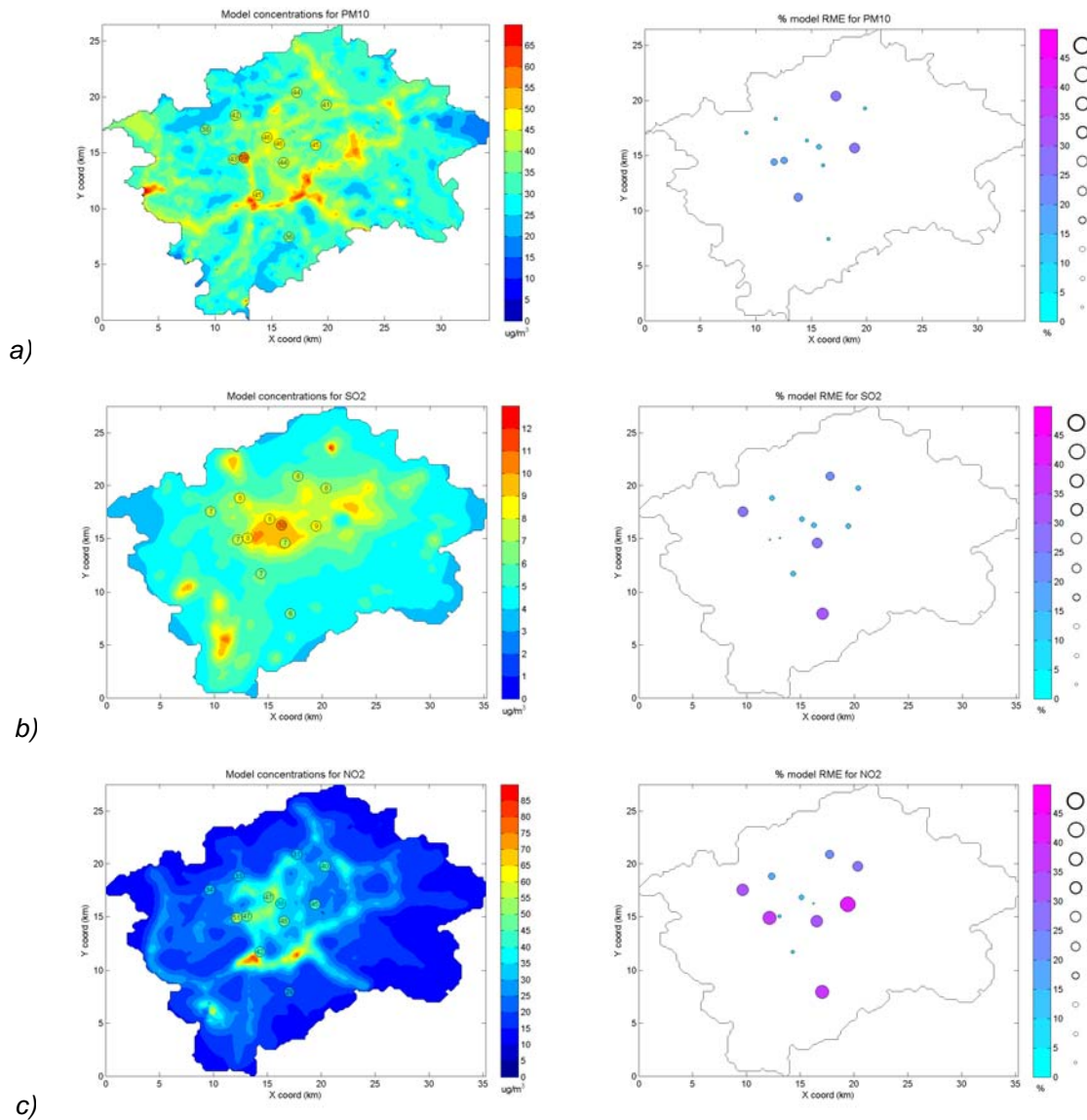


Figure 4.10: Spatial representation of RME (%) as individual points in space for a) PM<sub>10</sub>, b) SO<sub>2</sub> and c) NO<sub>2</sub>. Maps shown are the original model concentrations, left, and the RME representation, right. Dots are both colour and size coded for a clear indication of their value.

## 4.9 Probability of exceedance maps

By combining the concentration and the uncertainty maps, figures 4.6 – 4.8, it is possible to derive a map showing the probability of exceedance, given some limit value (LV), as described in section 3.6, using EU directive annual mean limit values. Plots of POE for PM<sub>10</sub> and NO<sub>2</sub> are shown below in figure 4.11. These are based on the initial model concentration and uncertainty fields, figures 4.6a – 4.8d, and on the Bayesian assimilated and uncertainty fields, figures 4.6d - 4.8d.

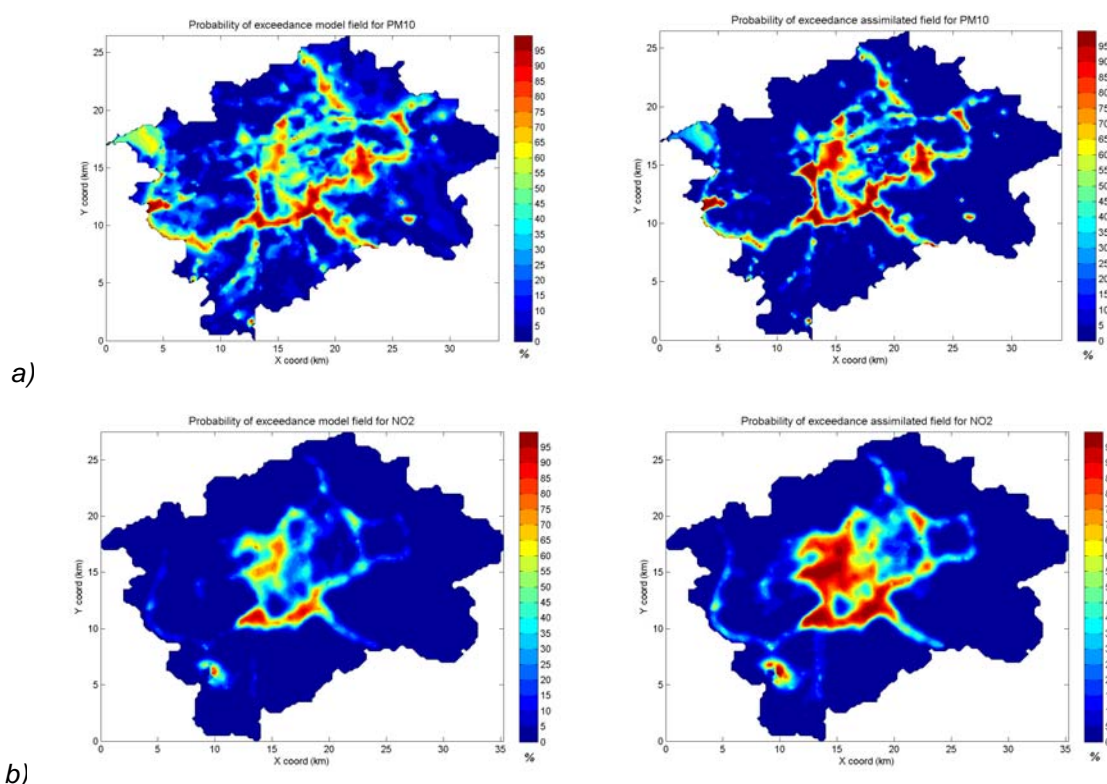


Figure 4.11: Probability of exceedance fields for 2003 in Prague for PM<sub>10</sub> (a) and NO<sub>2</sub> (b). The limit value for human health, EU daughter directive, for both pollutants is 40 µg/m<sup>3</sup>. The maps on the left are based on the original model calculations, the maps to the right based on the Bayesian assimilation method.

It is interesting to look at the differences in the total area where the limit values are exceeded for the original model calculations and for the assimilated calculations. In table 4.7 the portion, in percent, of the model domain that has a POE > 50% and 85% is shown for both PM<sub>10</sub> and NO<sub>2</sub>. Traditionally it is assumed that exceedance occurs when the POE is above 50%. For PM<sub>10</sub> the 50% exceedance area is slightly smaller for the assimilated fields, for NO<sub>2</sub> the area is significantly larger for the assimilated field. In contrast the region where exceedances are more certain to occur, i.e. POE > 85%, the area increases dramatically for NO<sub>2</sub> but only slightly for PM<sub>10</sub> with the application of assimilation.

Table 4.7: Relative area of the model domain with probability of exceedance greater than 50% and 85% for both the original model field and the Bayesian assimilated field.

Probability of exceedance above a threshold as % model area				
Method	PM <sub>10</sub>		NO <sub>2</sub>	
Map	Model	Assim	Model	Assim

% Model domain with POE > 50%	13.9 %	10.3 %	3.9 %	10.6 %
% Model domain with POE > 85%	1.8 %	2.9 %	0.3 %	3.5 %

## 5. Conclusion and discussion

### 5.1 Assessment of the case study

A case study that looks at a number of basic assimilation methods that combine monitoring and modelling has been carried out. The study investigated maps of annual mean concentrations of PM<sub>10</sub>, SO<sub>2</sub> and NO<sub>2</sub> for Prague in 2003. The original model fields were taken from the ATEM model and combined with data from 12 monitoring sites within the city of Prague.

A number of basic assimilation methods were tested including various forms of linear regression, kriging, differing forms of residual kriging and a Bayesian combination of kriged and model fields. The quality of the assimilation was assessed using cross validation of the RMSE. In addition to improved assimilated maps of concentrations, uncertainty and probability of exceedance maps were also calculated and shown.

The results indicate that simple methods such as linear regression can be used to improve the spatial concentration fields given a sufficient number of representative monitoring stations are available. It is not absolutely clear how many stations may be required but upward of 10 stations would seem necessary for robust conclusions to be drawn.

The case study also addresses the use of kriging and residual kriging on the urban scale. It was shown that there is little spatial correlation between monitoring stations to be able to clearly define the semi-variogram parameters required to carry out the kriging interpolation. Instead the more pragmatic approach of tuning the variogram model parameters to achieve the minimum cross validation RMSE was chosen as the most objective and efficient method under these situations. That there is limited spatial correlation between monitoring stations is indicative of the spatial variability on the urban scale since there can be large variations in concentrations on scales smaller than the typical distance between monitoring stations.

An alternative method to residual kriging was also applied, based on the Bayesian combination of kriged and modelled fields. This methodology takes into account the spatially distributed uncertainty in both observed and modelled fields and provides results similar to the other methods applied.

The most significant improvement in all the assimilation methods is the removal of the general model bias and this must be seen as the first and most important step in improving model results. General model bias can be the result of a number of modelling aspects including incorrect regional background contributions, incorrect emission factors, internal model bias or bias in meteorological parameters.

All these methods can be assessed using standard software applications available to city authorities and so represent operational methods for improving the spatial assessment of pollutants.

### 5.2 Improvements in assessment derived from case study

This case study has brought improvements in the following areas.

1. Allowed the identification of simple methods for improving model concentrations fields and their uncertainty using observational data
2. Has discussed and suggested methods for producing uncertainty maps attached to these concentrations fields and has produced uncertainty maps to help visualise the improvement obtained using the differing assimilation methods

3. Has assessed the improvement through the cross validation RMSE
4. Has shown that spatial interpolation of uncertainty parameters such as RME is not useful when the station density is not high and that these types of parameters should be shown as points
5. Has produced maps displaying the probability of exceedance

### **5.3 Recommendations resulting from the case study**

A number of recommendations resulting from this case study can be identified.

1. Basic methods such as linear regression, scaling or correction of bias using observations can significantly improve model results and their associated uncertainty. Which form of regression to be used depends on the availability of observational data.
  - a. When a large number of observational stations are available, the observed concentrations cover a wide range and correlation coefficients are significant then general linear interpolation can be used to improve model fields
  - b. When regional background concentrations are uncertain and correlation coefficients are low then correcting the mean bias can significantly improve results
  - c. When the regional background concentrations are well known but correlation is poor then fitting a linear regression that is forced to pass through the background value is recommended.
2. Kriging of observational data alone can give statistically better results than models but the uncertainty in these is very high, especially far from the observations. In addition kriging on the urban scale cannot capture the spatial variation that occurs on scales smaller than the station spacing. This limits the usefulness of both kriging and residual kriging on the urban scale.
3. The application of Bayesian assimilation methods is a recommended method to reduce the uncertainty in the spatial field in conjunction with linear regression.
4. To aid any modelling or assimilation method on the urban scale good knowledge of regional background concentrations is useful. When planning monitoring networks both high concentration hotspots as well as low concentration regions should be monitored.

### **5.4 Suitability for implementation in other cities**

The methodologies described in this case study are most suitable for cities that have a substantial monitoring network, i.e. 10 or more stations. Though in principle the simpler methods, such as correcting for bias, can be applied with very few stations the uncertainty will not necessarily decrease as a result. However just knowing the regional contribution with more certainty would help improve the results. Application of the methodologies require observations and model data that have the same spatial representativeness and this must be assessed before such a methodology can be applied.

## **References**

Air4EU – CS D7.1.7: Comparisons of data assimilation methods at urban scale in Paris

[http://www.air4eu.nl/reports\\_products.html](http://www.air4eu.nl/reports_products.html)

Air4EU – CS D7.1.10: Uncertainty in AQ assessment in London

[http://www.air4eu.nl/reports\\_products.html](http://www.air4eu.nl/reports_products.html)

Air4EU – CS D7.1.13: Basic data assimilation: application to the European scale

[http://www.air4eu.nl/reports\\_products.html](http://www.air4eu.nl/reports_products.html)

Air4EU – M5: Data assimilation

[http://www.air4eu.nl/reports\\_products.html](http://www.air4eu.nl/reports_products.html)

Brechler, J., 2000. Model assessment of air pollution in Prague. *Environmental monitoring and assessment* **65**: 269-276.

Cressie, N. (1993). *Statistics for Spatial Data (Revised Edition)*. Wiley: New York

Blond, N., L. Bel, and R. Vautard (2003), Three-dimensional ozone data analysis with an air quality model over the Paris area, *J. Geophys. Res.*, 108(D23), 4744.

Denby B., Flicstein B., 2005. Air quality now-cast system for the township of Haifa, Israel. *Proceedings of the Fifth international conference on Urban Air Quality, Valencia*. Published by University of Hertfordshire, CD-ROM, R.S. Sokhi, M.M. Milan and N. Moussiopoulos (eds.)

EC (1999). First Daughter Directive, Council Directive 1999/30/EC, relating to limit values for sulphur dioxide, nitrogen dioxide and oxides of nitrogen, particulate matter, and lead in ambient, OJ L 163, 29.06.1999, 41-60.

[http://eur-lex.europa.eu/LexUriServ/site/en/oj/1999/l\\_163/l\\_16319990629en00410060.pdf](http://eur-lex.europa.eu/LexUriServ/site/en/oj/1999/l_163/l_16319990629en00410060.pdf)

EC (2002). Third Daughter Directive, Council Directive 2002/3/EC, relating to ozone in ambient air, OJ L 67, 09.03.2002, 14-30.

[http://eur-lex.europa.eu/pri/en/oj/dat/2002/l\\_067/l\\_06720020309en00140030.pdf](http://eur-lex.europa.eu/pri/en/oj/dat/2002/l_067/l_06720020309en00140030.pdf)

Horálek, J., KurFurst, P., Denby, B., De Smet, P., De Leeuw, F., Brabec, M., and Fiala, J. (2005). Interpolation and assimilation methods for European scale air quality assessment and mapping, Part II: Development and testing new methodologies, *ETC/ACC Technical Paper 2005/8*.

[http://air-climate.eionet.europa.eu/reports/ETCACC\\_TechPaper\\_2005\\_8\\_Spatial\\_AQ\\_Dev\\_Test\\_Part\\_I](http://air-climate.eionet.europa.eu/reports/ETCACC_TechPaper_2005_8_Spatial_AQ_Dev_Test_Part_I)

Kasstele, van de J., R. B. A. Koelemeijer, A. L. M. Dekkers, M. Schaap, C. D. Homan and A. Stein (2006) Statistical mapping of PM<sub>10</sub> concentrations over Western Europe using secondary information from dispersion modelling and MODIS satellite observations. *Stoch Environ Res Risk Assess*, Vol 21, pp. 183–194

Webster, R. and Oliver, M.A., (2001). *Geostatistics for Environmental Scientists*. John Wiley & Sons.